ELSEVIER

Pattern Recognition Letters 23 (2002) 557–567

Pattern Recognition Letters

www.elsevier.com/locate/patrec

A parallel fuzzy scale-space approach to the unsupervised texture separation

M. Ceccarelli [a], A. Petrosino [b,*]

[a] *Universitá del Sannio, Via Port'Arsa 11, I-82100 Benevento, Italy*
[b] *CPS, National Research Council, Complesso Monte S. Angelo, Via Cintia, I-80126 Naples, Italy*

Received 16 October 2000; received in revised form 18 September 2001

Abstract

In this paper we consider the problem of unsupervised boundary localization in textured images reporting a parallel texture separation algorithm which extracts textural density gradients by a nonlinear multiple scale-space analysis of the image. The scale-space analysis is modeled by a differential morphological filter, and texture boundaries are extracted by segmenting the images resulting from a multiscale fuzzy gradient operation applied to the detail images, which are the differences between images at successive scales. Experiments and comparisons on Brodatz real textures are reported.

Keywords: Texture separation; Nonlinear scale space; Fuzzy gradient

1. Introduction

Texture analysis plays a fundamental role in computer vision. It has involved a huge amount of research in the last decades and has many fields of application such as aerial and satellite segmentation, ground classification, mineral analysis, industrial inspection and biomedical image analysis. The goal of texture analysis is to extract intrinsic features of texture to be used as image measures in the classification stage. The classification stage can be either supervised or unsupervised. In the first case the application domain and a set of reference images must be known. On the contrary, unsupervised methods make use of clustering techniques to discover the statistical differences between textural features.

Three principal approaches to texture analysis can be identified:

- *Statistical.* These approaches characterize the texture by the statistical relationships between neighboring pixels. They include eigenfilter, co-occurrence matrix, auto-regressive moving average, Markov Random Fields, Gaussian–Markov Random Fields, fractal dimensions.
- *Spectral.* These techniques are based on the response of the input image to a set of heuristically

* Corresponding author. Tel.: +39-081-5904253; fax: +39-081-5904219.
E-mail addresses: ceccarelli@unisannio.it (M. Ceccarelli), alfredo@ventotene.dma.unina.it (A. Petrosino).

0167-8655/02/$ - see front matter
PII: S0167-8655(01)00151-9

or optimized linear filters such as Gabor Filters, wavelet packets, difference of Gaussian, etc. Suitable nonlinear transformations are then applied in order to normalize and separate a set of filter responses.

- *Structural.* These methods rely on formal description of texture primitives either through grammar rules or by morphological representations.

In all such approaches a common factor is the concept of *scale* which is related to the unknown mean size of texture primitive (''texels''). The use of multiple scales can be of aid when facing complex pattern recognition problems such as texture separation. Indeed a scale-space analysis of an image is a family of smoothed images derived on the basis of a continuous scale parameter (Badaud et al., 1986; Jackway and Deriche, 1996; Koenderink, 1984). As the scale increases the image get coarser and fine details are gradually suppressed. The meaningful features in the original signal, which persist at higher scales, can be then identified by following their path in the resulting scale-space. Although early works on scale-space were essentially based on linear filtering using the Gaussian function as smoothing kernel (known as Gaussian Pyramid (Burt, 1981)), it is now recognized that even nonlinear filters such as multiscale dilation and erosion can posses the monotonic property for signal extrema which is the fundamental requirement of continuous scale-space analyses (Brockett and Maragos, 1994; Jackway and Deriche, 1996). The main advantage of using these last filters is that they do not cause features to be shifted by smoothing. In addition, the morphological approach to texture analysis has proven to be an efficient tool for textural feature extraction and description (Dougherty et al., 1992; Petreux and Schmitt, 1988). These morphological approaches to texture analysis mainly rely on a level-set based representation of the input images. The processing of level sets can be carried out to extract meaningful information from the image such as mean size of the texels in the ''Granold theory'' (Jones and Jackway, 2000) or structural property of the texture, which can be used for example to synthesize similar images (Gousseau and Morel, 2000).

The concept of multiscale image analysis is incorporated at two different stages of the texture segmentation method we propose: (a) a continuous morphological filtering modeled by a diffusion equation, where the scale parameter is the ''time'' variable of the diffusion, as described in Section 2; (b) the morphological analysis for extracting gradient images, where the scale parameter is the window size of the local fuzzy gradient operator, which is derived by the integration of fuzzy set theory (Zadeh, 1965) and the rough theory (Pawlak, 1982), as described in Section 4. After the two-stages analysis, boundary localization is then performed by clustering a multichannel image composed by a set of multiscale fuzzy gradient images.

The paper is organized as follows. Section 2 reports the adopted multiscale representation, whereas Sections 3 and 4, respectively, report the textural gradient features which we use for separation. Finally, in Section 5 we present the experimental results on real textures.

2. Non-linear scale-space filtering

A morphological *scale-space* representation of an image $u_0(\boldsymbol{x}), \boldsymbol{x} \in \Re^2$, is defined as a family of smoothed images, derived on the basis of a scale parameter t, i.e., given $u_0(\boldsymbol{x}), u(\boldsymbol{x}, t)$ means the ''image u_0 analyzed at scale t''. The *Affine Morphological Scale Space* (AMSS) model, introduced in (Alvarez et al., 1993), is defined as the solution of the following second-order nonlinear partial differential equation:

$$\frac{\partial u}{\partial t} = |\nabla u|(\mathrm{curv}(u))^{\frac{1}{3}} \quad u(\boldsymbol{x}, 0) = u_0(\boldsymbol{x}), \tag{1}$$

where $\mathrm{curv}(u)$ represents a second-order differential operator corresponding to the curvature of level curves of $u(\boldsymbol{x}, t)$, i.e.,

$$\mathrm{curv}(u) = \frac{u_{xx}u_y^2 - 2u_{xy}u_x u_y + u_{yy}u_x^2}{(u_x^2 + u_y^2)^{3/2}}.$$

Here the notation u_x represents the partial derivative of u with respect to the variable x and analogously for the other differential operators.

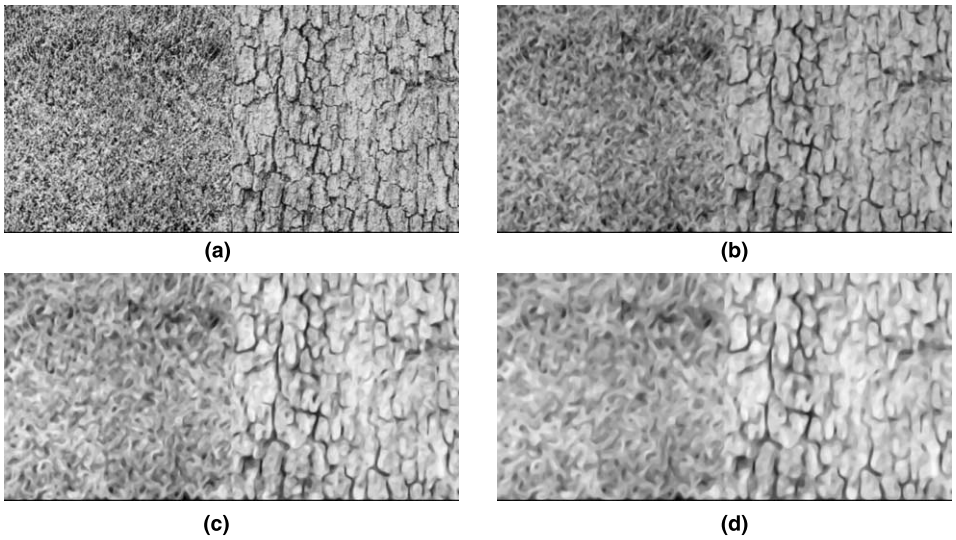

Fig. 1. A textured image at different scales: $t = 0$ (a); $t = 1.0$ (b); $t = 2$ (c) and $t = 3$ (d).

This kind of smoothing possesses invariance properties; specifically, the model (1) is the unique multi-scale analysis which has the properties of:

- *Contrast invariance*. We perceive textures on the basis of relative spatial relationships between pixels, rather than the luminosity itself. This means that a filtering process aimed at analyzing textures should be invariant to changes which preserve the relative order of luminance values. In particular, a *contrast change* of an image $u(\boldsymbol{x})$ is the application to u of any increasing function, eventually nonlinear; a contrast invariant filter operates just on the level curves of the image.
- *Rotation and translation invariance*, as we perceive textures independently of position and orientation.
- *Affine stretching invariance*, as our perception of textures is influenced by stretching (Julesz, 1986), i.e., discrimination of textures can be reduced by stretching the individual textons. Therefore, the invariance to this operation can preserve the perception of the original texture. Unfortunately, the invariance to general stretching is difficult to be formally imposed. However, linear stretching corresponds to an affine transformation and the model expressed by Eq. (1) has been shown by Alvarez et al. (1993) to be invariant under affine transformations.

These properties allow the model (1) to preserve the structure of the textural patterns even at coarser scales; this is due to its geometrical behavior, which moves the level curves of the image with a speed proportional to their curvature (Evans and Spruck, 1991).

Starting from a textured image, a multichannel image can be built by using its smoothed versions generated through the iterative application of model (1). Fig. 1 reports a textured image analyzed at different scales. As it can be seen from the figure, the structure of the texture is preserved even at large scales. Indeed, the anisotropy of the filtering process tends to smooth out the level curves of the image, which eventually collapse into larger groups, but the shape of the curves which embeds the preferred orientation of the textures is maintained.

3. Detail images

The *detail images* provide information about how the level curves move during the evolution of

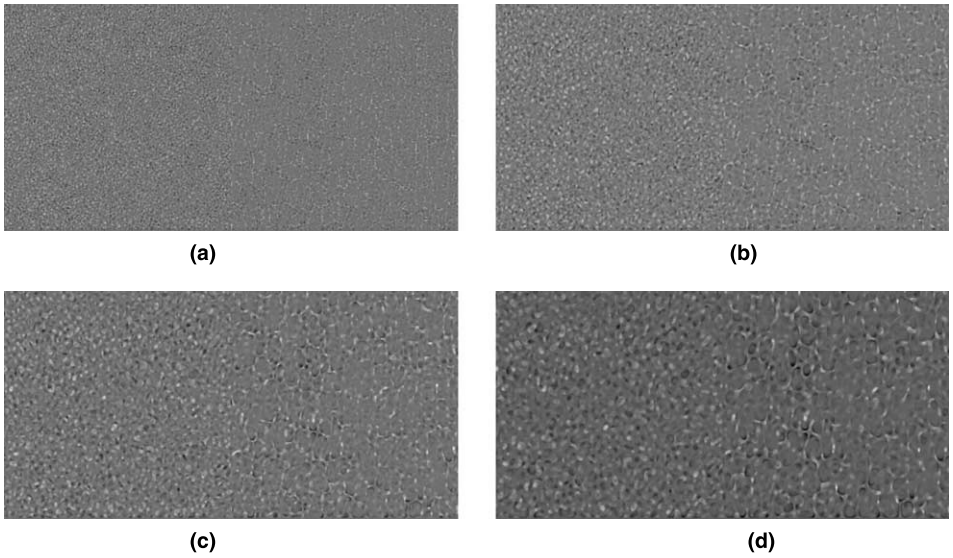

Fig. 2. The detail images corresponding to Fig. 1. The images have been obtained by applying Eq. (2) with a discretization step $\Delta t = 0.2$: (a) d_1, (b) d_5, (c) d_{10} and (d) d_{15}.

Eq. (1) and represent the structure of the textural patterns in terms of differences between the level curves at different "times". The detail images are obtained as differences between the images analyzed at successive scales

$$d_i(\boldsymbol{x}) = u(\boldsymbol{x}, t_i) - u(\boldsymbol{x}, t_{i-1}) \tag{2}$$

with the scale parameter t discretized at increasing values $t_0 = 0, t_1, t_2, \ldots, t_n$. Since the filtering process is influenced by the orientations of the textural patterns, i.e., the model expressed by Eq. (1) is anisotropic, we do not need to perform orientation selective smoothing.

The sequence of detail images corresponds to a representation of the motion of the level curves through time; some of these images are depicted in Fig. 2 computed over the sequence depicted in Fig. 1. These images have been obtained by applying Eq. (2) with a time discretization step $\Delta t = 0.2$. In particular, Fig. 2(a) is d_1, Fig. 2(b) is d_5, Fig. 2(c) is d_{10} and Fig. 2(d) is d_{15}.

The discrimination between textural patterns is performed by applying a multi-scale fuzzy gradient operation to each detail image followed by a hierarchical clustering algorithm as shown in the next section.

4. Morphological gradient images and segmentation

Here, we face the problem of analyzing the detail images in order to extract textural gradients which indicate the local change of structural relationships between neighboring pixels. To this purpose, we will use elements of the rough set theory (Pawlak, 1982) which is an extension of the set theory dealing with coarse information. Before proceeding into the details of the fuzzy gradient operator some background definitions are needed.

In the context of the rough set theory, a set $X = \{x_1, \ldots, x_n\}$ is approximated by two sets, called upper and lower approximations, respectively denoted by $\underline{C}(X)$ and $\overline{C}(X)$, such that $\underline{C}(X) \subseteq X \subseteq \overline{C}(X)$. These definitions are easily extended to fuzzy sets for dealing with uncertainty. Here we use a class of fuzzy rough sets introduced in (Apostolico et al., 1978; Caianiello and Petrosino, 1994). Let $\{x_1/\mu(x_1), \ldots, x_n/\mu(x_n)\}$ be a fuzzy set F on X defined by adding to each element of X the degree of its membership to the set through a mapping $\mu : X \to [0, 1]$. Basic operations on fuzzy sets F_1 and F_2 are union and intersection, respectively defined by $\mu_{F_1 \cup F_2} : x \in X \to \max\{\mu_{F_1}(x), \mu_{F_2}(x)\}$ and $\mu_{F_1 \cap F_2} : x \in X \to \min\{\mu_{F_1}(x), \mu_{F_2}(x)\}$. A

Composite set (*C*-set) (see Apostolico et al., 1978) is defined as a triple $C = (\Gamma, m, M)$, such that

- $\Gamma = \{X_1, \ldots, X_p\}$ is a partition of X into p disjoint subsets $X_1, \ldots, X_p$, i.e., $X_i \cap X_j = \emptyset,\ i \neq j$, and $\cup_i X_i = X$;
- let a membership function μ be defined over X to a fuzzy set F. m and M are mappings defined by

  $m(x) = m_k \quad \text{if } x \in X_k,$

  where $m_k = \inf\{\mu(y) \mid y \in X_k\}$, and

  $M(x) = M_k \quad \text{if } x \in X_k,$

  where $M_k = \sup\{\mu(y) \mid y \in X_k\}$;
- Γ and μ uniquely define a *C*-set;
- it holds

  $m(F) \subseteq F \subseteq M(F),$

  where $m(F)$ ($M(F)$) denotes the fuzzy set $\{x/m(x)\}$ ($\{x/M(x)\}$), i.e., the lower (upper) approximation of F.

In addition to usual operations defined over fuzzy sets, like union and intersection, a basic operation is valid over Composite sets, called *C-product*. The *C*-product operation between couples of *C*-sets is defined as follows. Given two sets C and C', both related to different partitions of the same set X, the *C*-product, denoted by $\otimes$, is defined as a new *C*-set C'':

$$C'' = C \otimes C' = (\Gamma'', m'', M''),$$

where Γ'' is a new partition whose elements are the sets

$$\Gamma''_{k,l} = X_k \cap X_l \quad \text{with } X_k \cap X_l \neq \emptyset$$

and $m''_{k,l} = \max\{m_k, m'_l\},\ M''_{k,l} = \min\{M_k, M'_l\}$. The *C*-product satisfies:

$$m(F) \subseteq m''(F) \subseteq F \subseteq M''(F) \subseteq M(F)$$

and

$$m'(F) \subseteq m''(F) \subseteq F \subseteq M''(F) \subseteq M'(F).$$

As shown in (Dubois and Prade, 1990) this computation scheme generalizes the concept of fuzzy set to rough fuzzy set. It has been also demonstrated in (Apostolico et al., 1978) that recursive application of the previous operation provides a refinement of the original sets, realizing a powerful tool for measurement and a basic signal processing technique. Edge detection, gray-level image segmentation and image coding have been performed by combining the low-level analysis provided by these operations together with fuzzy classification (Caianiello and Petrosino, 1994; Petrosino, 1996). Recently, it has been shown that there is a tight relationship between rough sets and mathematical morphology (Bloch, 2000). For a good comprehensive survey of successful applications of fuzzy theory and rough theory to image processing refer to Kerre and Nachtegael (2000).

On the basis of the above definitions, let us explain how we apply the above theory to the extraction of *textural gradients* in image analysis. Let us consider to have computed a set (in terms of different scale factors of the AMSS model) of detail images according to Eq. (2).

Let now X denote the set of pixel positions, i.e., X is the Cartesian product $\{0, \ldots, N-1\} \times \{0, \ldots, M-1\}$, i.e., the image size is $N \times M$. Let us define as fuzzy membership function μ over X the function that associates to each pixel $x \in X$ the value

$$\mu(\boldsymbol{x}) = d(\boldsymbol{x}),$$

i.e., μ is the value of a specific detail image d attained at pixel location $\boldsymbol{x}$. This means that d is a fuzzy measure of the image change between successive scales.

Since local properties can be extracted by a multiresolution mechanism realized on the basis of the theory of the *C*-sets (Petrosino, 1996), let us consider a partition Γ^1, composed of all the non-overlapping windows of size $w \times w$. Boundary conditions are dealt with symmetric reflections of the border rows and columns. A second partition, Γ^2 can be obtained by shifting Γ^1 on the right of $w-1$ pixels. According to this way of doing, each element of the partition Γ^2 intersects a column containing w pixels of an element of the partition Γ^1. Following this construction, other two partitions, Γ^3 and Γ^4, can be obtained by respectively shifting Γ^1 and Γ^2 downward of $w-1$ pixels. Each pixel of the image can be seen as the intersection of four corresponding elements of the partitions $\Gamma^1,\ \Gamma^2,\ \Gamma^3,\ \Gamma^4$, as shown in Fig. 3.

As previously introduced each partition $\Gamma^i, i = 1, \ldots, 4$ can be associated to a *C*-set $\mathscr{C}^i = (\Gamma^i, m_i, M_i)$. According to the previously

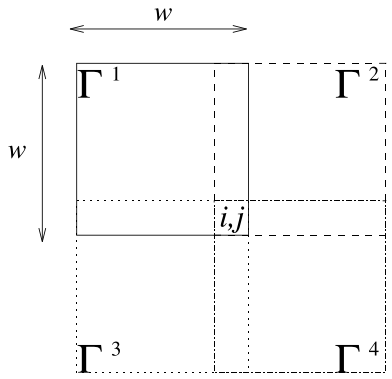

Fig. 3. Each image pixel can be seen as the intersection of four elements of the partitions Γ^1, Γ^2, Γ^3, Γ^4.

defined C-product operation, each pixel can be seen as belonging to the partition obtained by "C-producting" the original four C-sets:

$$\mathscr{C} = \mathscr{C}^1 \otimes \mathscr{C}^2 \otimes \mathscr{C}^3 \otimes \mathscr{C}^4. \tag{3}$$

According to these operations, the unique parameter is the size of each partition element w, which represents the *scale* of the multiscale mechanism to get textural gradient features from the detail images computed as described in the previous section. Therefore, we have a two stage multiscale analysis based on the parameters t and w. The first is used to get a sequence of detail images, which are the differences between images at successive t scales, while the second stage, which extracts a textural gradient, depends on the window size w, also considered as a scale parameter.

In particular, the *multiscale gradient* definition based on the previous operations holds:

Definition 1. Given the maxima and minima images (respectively M and m) generated by the application of the operation (3) over four different partitions of an image, each element of size w, the *multiscale gradient* of the image at a scale w computed at each position (i,j), is defined as

$$G^w_{i,j} = M^w_{i,j} - m^w_{i,j}. \tag{4}$$

Therefore, this operation corresponds to the difference between the lower and upper approximation of a fuzzy set. To extract texton gradient information at different scales, the gradient operation (4) has to be applied to all the detail images obtained from (2), by using increasing values of w and generating a multichannel image to be segmented. This means that we first perform a nonlinear smoothing depending on the parameter t, which at the first stage represents the scale of the smoothed image, and then apply the fuzzy gradient operation to all the images d_i which are the differences between images at successive scales. This last fuzzy gradient operation also depends on another scale parameter: the window size w. For the sake of clearness, the algorithm of Fig. 6 reports the steps of the proposed method. As an example, Fig. 4 reports the images corresponding to the application of Eq. (4) for different window sizes w to some of the detail images depicted in Fig. 2. Indeed, on the boundary between textures there is a change of local homogeneity of the gradient images.

Here, we adopt the parallel segmentation algorithm described in (Petrosino and Ceccarelli, 2000). It is a stochastic region growing algorithm for multichannel images based on standard agglomerative clustering (Duda and Hart, 1973). It is aimed at the minimization of a cost functional consisting of two terms: the first is represented by the within-cluster variance, whereas the second is a complexity term counting the length of the boundary among clusters (LeClerc, 1989; Mumford and Shah, 1989).

5. Experiments and comparisons

In this section we present some experiments for the quantitative assessment of the performance. Firstly, let us show the behavior of the algorithm on a pair of texture images. In this paper we have reported the various steps of the proposed method also summarized in Fig. 6. In particular, in Fig. 1 we can find the images analyzed at different scales t, in Fig. 2 we find the corresponding detail images, whereas in Fig. 4 we have reported the fuzzy gradient images corresponding to different window size parameters w. As the images of Fig. 4 show, the fuzzy gradient operation is aimed to the detection of discontinuities in the

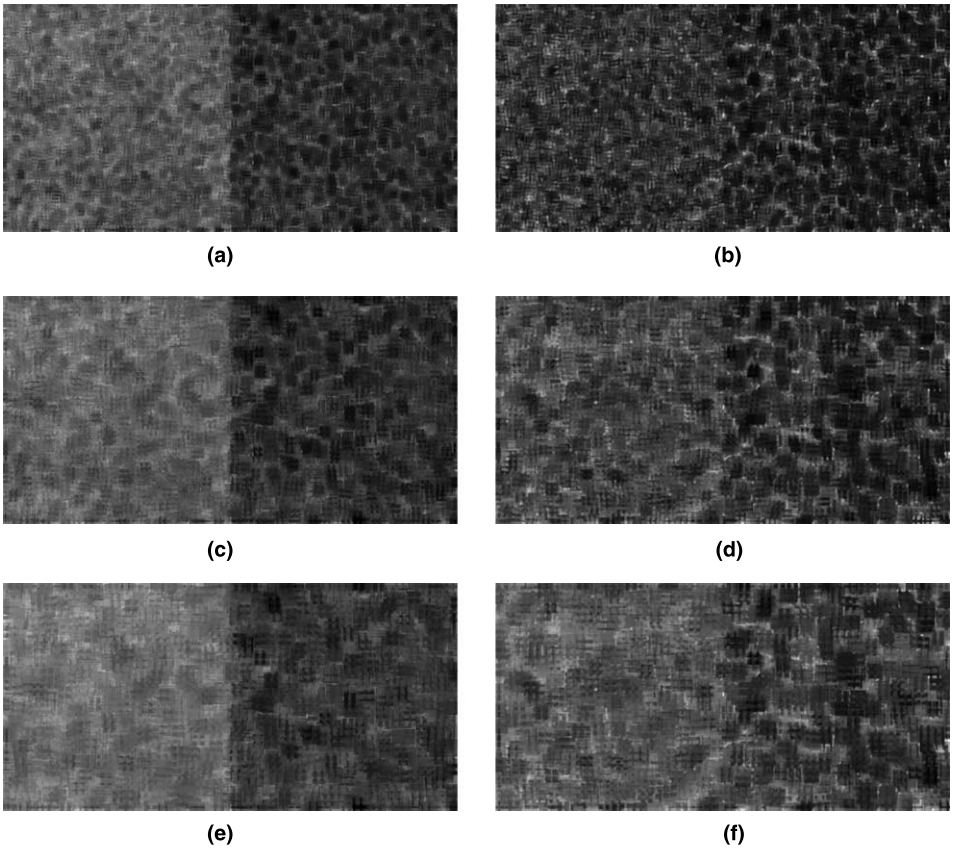

Fig. 4. The fuzzy gradient images with parameter values: (a) $w = 5, t = 0$, (b) $w = 5, t = 2$, (c) $w = 7, t = 0$, (d) $w = 7, t = 2$, (e) $w = 9, t = 0$, (f) $w = 9, t = 2$.

sequence of details. Indeed, on the boundary between textures there is a change of local homogeneity of the gradient images. The variational region growing algorithm, reported in (Petrosino and Ceccarelli, 2000), produces the result depicted in Fig. 5 where the two textures are efficiently separated.

Fig. 5. The segmented image of Fig. 4.

In order to perform a quantitative assessment of the algorithm, and bringing in mind the aim of texture separation, rather than texture classifica-

for $i = 0$ **to** n
  compute $u(\cdot, t_i)$ according to (1)
end for
for $i = 1$ **to** n **do**
  // compute the detail images: //
  $d_i(\cdot) = u(\cdot, t_i) - u(\cdot, t_{i-1})$
  for $w = w_{in}$ **to** w_{fin} **increment by** Δw **do**
    // compute multiscale texton gradients according to (4): //
    $G^w(d_i) = M^w(d_i) - m^w(d_i)$
  end for
end for
// Assemble the $n \cdot \frac{w_{fin} - w_{in}}{\Delta w}$ *texton gradient images //*
Segment the multichannel image.

Fig. 6. Texture discrimination algorithm.

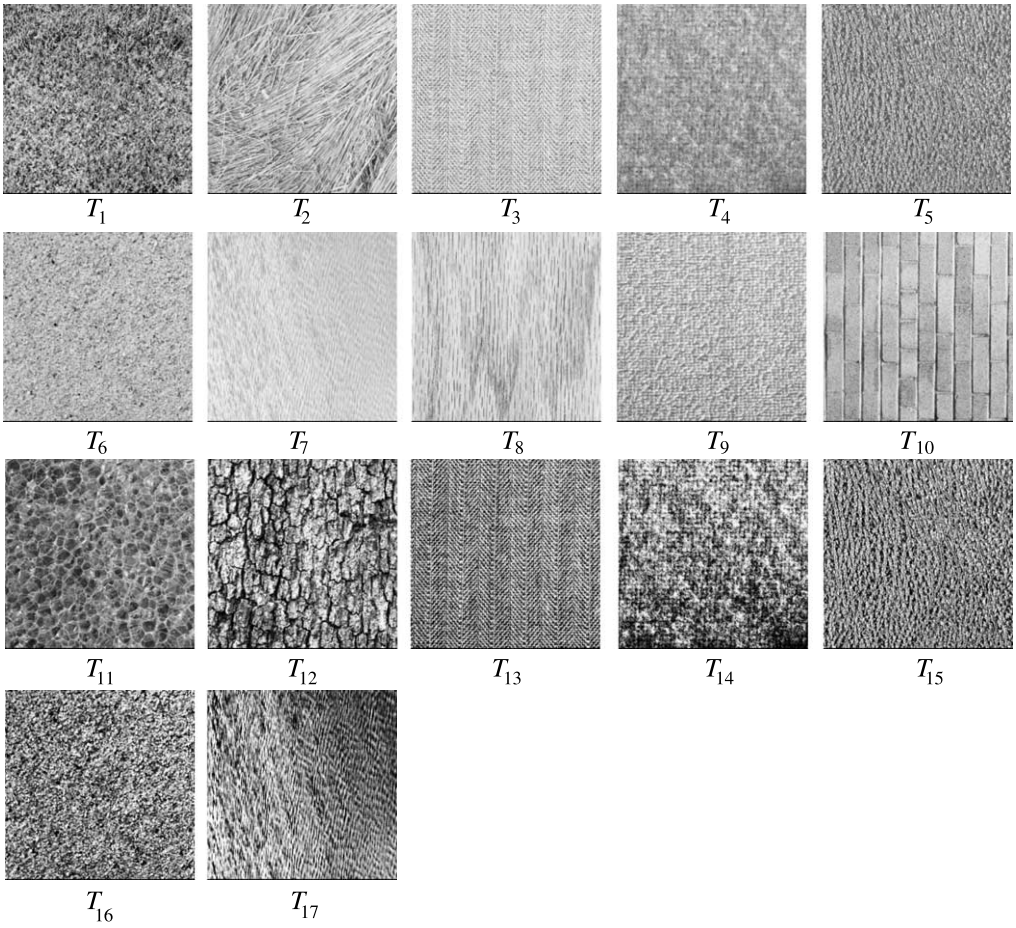

Fig. 7. The 17 Brodatz textures used for the performance analysis.

tion, we have applied the proposed method to a set of images containing pairs of Brodatz textures. In particular, our test set consists of the 17 textures depicted in Fig. 7 each of size 256×256. The algorithm has been applied to 272 different images each constructed by aligning two textures of the test set along the horizontal direction. Fig. 1(a) is an example of such images. In order to evaluate the separation error we adopted the following procedure. The connected components of the segmented image are first labeled by using an adaptation of the relabeling algorithm reported in (Tsao et al., 1994) to the case of a two-class problem, then the Hamming distance between the labeled image and the truth image depicted in Fig. 8 is computed as a measure of the error. The

Fig. 8. The truth image.

error percentages, relative to the image size, for all the considered textures are reported in Table 1. The input images in this experiments were analyzed at scales between 0 and 3 with an interval between scales for the computation of the detail

Table 1
Matrix of error percentages, each entry indicating the relative difference between the segmentation of an image containing two textures and the truth image

	T_1	T_2	T_3	T_4	T_5	T_6	T_7	T_8	T_9	T_{10}	T_{11}	T_{12}	T_{13}	T_{14}	T_{15}	T_{16}	T_{17}	Average
T_1	0.0	2.5	0.3	0.0	2.1	0.3	0.0	0.5	0.3	0.2	0.3	1.0	0.3	2.0	0.3	0.1	2.0	0.7
T_2	0.6	0.0	51.2	0.3	5.8	1.3	0.4	0.8	1.7	0.8	1.6	0.8	0.1	0.6	0.1	0.1	0.6	3.9
T_3	0.4	49.8	0.0	0.1	2.3	0.6	0.1	0.3	12.5	0.3	3.7	0.5	0.0	0.2	0.2	0.2	0.5	4.2
T_4	0.0	0.4	0.3	0.0	0.2	2.7	2.5	49.7	0.5	1.6	2.0	0.0	0.0	0.2	0.0	0.0	0.5	3.6
T_5	0.6	49.8	5.0	0.1	0.0	0.5	0.1	0.6	0.5	0.1	0.7	0.6	0.4	0.3	0.1	0.1	0.7	3.5
T_6	0.2	1.1	0.4	2.4	0.3	0.0	0.8	5.4	4.1	1.1	49.9	0.1	0.2	0.2	0.1	0.0	0.2	3.9
T_7	0.0	0.0	0.0	0.1	0.0	0.1	0.0	2.5	0.4	50.0	0.0	0.0	0.0	0.1	0.0	0.0	0.8	3.2
T_8	0.3	0.5	0.2	50.1	0.7	0.9	7.9	0.0	0.4	4.5	0.3	0.2	0.0	0.3	0.1	0.0	0.5	3.9
T_9	0.3	2.8	2.7	0.3	0.5	10.8	0.2	0.3	0.0	0.6	50.0	0.0	0.0	0.5	0.1	0.0	0.2	4.1
T_{10}	0.4	0.3	0.4	1.0	0.4	0.8	50.0	50.0	1.0	0.0	1.1	0.0	0.0	0.2	0.0	0.0	0.4	6.2
T_{11}	0.3	1.8	2.1	1.2	0.7	50.1	0.4	0.5	50.1	0.8	0.0	0.1	0.0	0.2	0.1	0.0	0.3	6.4
T_{12}	50.5	0.9	0.3	0.0	1.0	0.2	0.0	0.1	0.2	0.1	0.2	0.0	0.2	49.7	0.4	1.1	2.9	6.3
T_{13}	0.0	0.0	0.0	0.0	0.0	0.0	0.0	0.0	0.1	0.0	0.0	0.3	0.0	0.2	0.9	0.6	37.6	2.3
T_{14}	4.4	1.7	1.7	0.4	2.0	1.3	0.0	0.4	1.2	0.6	1.3	51.1	0.6	0.0	0.6	1.0	3.0	4.2
T_{15}	0.8	0.0	0.0	0.1	0.0	0.0	0.0	0.0	0.0	0.1	0.0	1.5	1.0	3.8	0.0	49.8	35.7	5.5
T_{16}	0.8	0.0	0.0	0.0	0.0	0.0	0.0	0.0	0.0	0.0	0.0	1.5	0.9	1.2	50.3	0.0	35.9	5.3
T_{17}	13.5	3.2	2.2	0.3	3.5	0.6	0.1	0.6	0.9	0.1	2.4	14.5	0.3	14.6	0.2	0.5	0.0	3.4
Average																		4.2

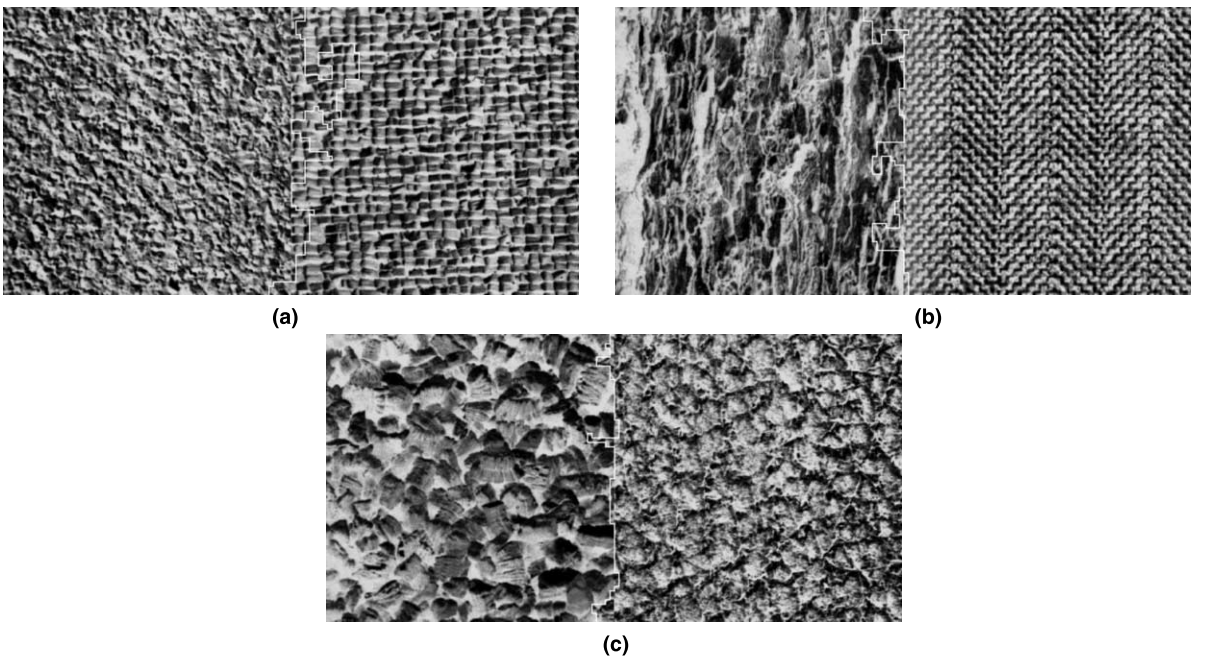

Fig. 9. Three images containing pairs of textures reported in (Randen and Husoy, 1999) with the superimposed segmentation obtained by the proposed method.

images of 0.5; therefore, for each image we obtain five detail images. The fuzzy morphological gradient operation was then applied with window dimensions $w = 5, 7, 9$, giving rise to a multichannel image to be segmented with $3 \times 5 = 15$ layers (refer to the algorithm of Fig. 6).

Considering the enormous amount of research done in the field of texture analysis and the number of proposed approaches, the comparison with other algorithms is a very difficult task. Recently, in (Randen and Husoy, 1999), a comparative study regarding the performance of a large number of textural filtering methods for classifying a set of test images (made available by the authors) has been reported. To make the comparisons, the proposed methods have been applied to the images of two adjacent textures as reported in (Randen and Husoy, 1999) and depicted in Fig. 9. The obtained results, reported in Table 2, assert the best performance achieved by our method. For the sake of clearness, we point out that the results in (Randen and Husoy, 1999) have been obtained by using a supervised classification algorithm, namely the Learning Vector Quantization (LVQ), applied to each multichannel pixel of the filtered images. On the contrary, our segmentation algorithm is completely unsupervised requiring just the specification of the number of regions in the final segmentation. However, as a region growing algorithm does, it does not perform a classification of each pixel, rather it agglomerates regions containing similar pixels. We underline that all the computational steps of the proposed method are based on local operators, therefore the algorithm can be easily mapped on fine-grained parallel machines, such as for instance the Associative Meshes described in (Merigot, 1997).

Table 2
Error percentages with various filtering methods for the images of Fig. 8, see Randen and Husoy (1999) for the details of each method

Eigenfilter	4.1
Opt. Rep. Gabor filter bank	15.8
Prediction error filter	12.9
Optimal Gabor filter $\sigma = 2$	8.2
Optimal Gabor filter $\sigma = 4$	6.7
Optimal Gabor filter $\sigma = 8$	7.9
Optimal Gabor filter $\sigma = 16$	17.3
4-filter opt. Gabor filter bank	8.9
6-filter opt. Gabor filter bank	8.2
10-filter opt. Gabor filter bank	6.3
J_{MS}	12.7
J_U	2.4
J_F	2.4
Backprop. NN mask size 11	35.2
Backprop. NN mask size 22	36.0
Proposed	2.20

6. Conclusions

We have reported a texture separation algorithm based on a nonlinear multiscale representation of the input image. Boundaries between homogeneous textured regions are extracted by segmenting a multichannel image generated by computing a multiscale fuzzy gradient operation applied to detail images. The reported experiments and the comparisons show the ability of the algorithm to separate pairs of real textures. The algorithm is completely unsupervised, and it requires just to a priori know the number of regions in the final segmentation; further studies will be aimed to overcome this drawback.

References

Alvarez, L., Guichard, F., Lions, P.L., Morel, J.M., 1993. Axioms and fundamental equations of image processing. Arch. Rational Mech. Anal. 123 (3), 199–257.

Apostolico, A., Caianiello, E.R., Fischetti, E., Vitulano, S., 1978. *C*-Calculus: an elementary approach to some problems in pattern recognition. Pattern Recognition 19, 375–387.

Badaud, J., Witkin, A., Baduin, M., Duda, R., 1986. Uniqueness of the Gaussian kernel for scale-space filtering. IEEE Trans. Pattern Anal. Machine Intell. 8, 26–33.

Bloch, I., 2000. On links on between mathematical morphology and rough sets. Pattern Recognition 33 (9), 1487–1496.

Brockett, R.W., Maragos, P., 1994. Evolution equations for continuous-scale morphological filtering. IEEE Trans. Signal Process. 42, 3377–3386.

Burt, P.J., 1981. Fast filters transforms for image processing. Comput. Graphics Image Process. 16, 20–51.

Caianiello, E.R., Petrosino, A., 1994. Neural networks, fuzziness and image processing. In: Cantoni, V. (Ed.), Machine and Human Perception: Analogies and Divergences. Plenum Press, New York, pp. 355–370.

Dougherty, E., Newell, J., Pelz, J., 1992. Morphological texture-based maximum likelihood pixel classification based on local granulometric moments. Pattern Recognition 25 (10), 1181–1198.

Dubois, D., Prade, H., 1990. Rough fuzzy sets and fuzzy rough sets. Int. J. General Syst. 17, 119–209.

Duda, R.O., Hart, P.E., 1973. Pattern Classification and Scene Analysis. Wiley, New York.

Evans, L.C., Spruck, J., 1991. Motion of level sets by mean curvature. J. Differential Geometry 33, 635–681.

Gousseau, Y., Morel, J.M., 2000. Texture synthesis through level sets. ENS Cachan-CMLA Internal Report.

Kerre, E.E., Nachtegael, M. (Eds.), 2000. Fuzzy Techniques in Image Processing. Springer, Berlin.

Koenderink, J., 1984. The structure of images. Biological Cybernet. 5, 363–370.

Jackway, P.T., Deriche, M., 1996. Scale-space properties of the multiscale morphological dilation-erosion. IEEE Trans. Pattern Anal. Machine Intell. 18 (1), 38–51.

Jones, D.G., Jackway, P.T., 2000. Granolds: a novel texture representation. Pattern Recognition 33, 1033–1045.

Julesz, B., 1986. Texton gradients: the texton theory revisited. Biological Cybernet. 54, 245–251.

LeClerc, Y., 1989. Constructing simple stable descriptions for image partitioning. Int. J. Comput. Vision 3 (1), 73–102.

Merigot, A., 1997. Associative nets: a graph-based parallel computing model. IEEE Trans. Comput. 48 (5), 558–571.

Mumford, D., Shah, J., 1989. Optimal approximations by piecewise smooth functions and associated variational problems. Commun. Pure Applied Math. 42, 577–685.

Pawlak, Z., 1982. Rough sets. Int. J. Inf. Comput. Sci. 11 (5), 341–356.

Petreux, F., Schmitt, M., 1988. Boolean texture analysis and synthesis. In: Serra, J. (Ed.), Image Analysis and Mathematical Morphology, Vol. 2. Academic Press, New York, pp. 377–400.

Petrosino, A., 1996. Rough fuzzy sets and unsupervised neural learning: applications in computer vision. In: Bonarini, A., Mancini, D., Masulli, F., Petrosino, A. (Eds.), New trends in Fuzzy Logic. World Scientific, Singapore, pp. 166–176.

Petrosino, A., Ceccarelli, M., 2000. Unsupervised texture discrimination based on rough fuzzy sets and parallel hierarchical clustering. In: Proc. IEEE Internat. Conf. on Pattern Recognition ICPR2000. IEEE Computer Society Press, Silver Spring, MD, pp. 1100–1103.

Randen, T., Husoy, J.H., 1999. Filtering for texture classification: a comparative study. IEEE Trans. Pattern Anal. Machine Intell. 21 (4), 291–310.

Tsao, E.C.K., Bezdek, J.C., Pal, N.R., 1994. Fuzzy Kohonen clustering network. Pattern Recognition 27, 757–764.

Zadeh, L.A., 1965. Fuzzy sets. Inf. Control 8, 338–353.